

it can be proved by substitution and simplification that

$$C_{Di} = 8 \frac{l}{s} \frac{l}{c} \int_0^{\pi/2} \sum_{n=1}^{\infty} B_n \sin n\theta_1 \sin\theta_1 \times \\ \left\{ \int_0^{\pi/2} \sum_{n=1}^{\infty} n B_n \cos n\theta \coth \frac{\pi l}{s} (\cos\theta - \cos\theta_1) d\theta - \right. \\ \left. \int_0^{\pi/2} \sum_{n=1}^{\infty} n B_n \cos n\theta \coth \frac{\pi l}{s} \times \right. \\ \left. (2 + 2\Omega - \cos\theta - \cos\theta_1) d\theta \right\} d\theta_1 \quad (13)$$

Numerical Results and Experimental Verification

A cascade of split compressor blades (10C4 30 C50-British Profile), whose lift angle-of-attack characteristic is known, was selected, and measurements of lift and induced drag were carried out at Reynolds number (with respect to chord) of 2×10^5 . The results so obtained are plotted in Fig 2.

Liverpool University DEUCE Computer has been used to evaluate induced drag coefficients theoretically, and the results are plotted and compared with experimental values in Fig 2.

Discussion and Conclusions

The agreement between theoretical and experimental values is reasonably good at high gap/chord ratios. At low gap/chord ratios, the real fluid effects inside the gap, the finite thickness, and chord length of the blade reduce leakage flow and, hence, the strength of the trailing vortices. This accounts for the poor agreement between the theoretical and experimental values at low gap/chord ratios. A modified analysis has been suggested for low gap/chord ratios, and this has been dealt with in Ref 1.

References

- ¹ Lakshminarayana, B., "Leakage and secondary flows in axial compressor cascades," Ph.D. Thesis, Liverpool Univ., Liverpool, England (1963).
- ² Milne-Thompson, L., *Theoretical Hydrodynamics* (Macmillan and Co. Ltd., London, England, 1960), Chap. 13.
- ³ Glauert, H., *Aerofoil and Airscrew Theory* (Cambridge University Press, Cambridge, England 1948), Chap. 11.

Location of Catch-Up Point in a ΔV Perturbed Circular Orbit

ANDREW H. MILSTEAD*

Aerospace Corporation, El Segundo, Calif

Introduction

REFERENCE 1 compares the position of a drag-free satellite in a circular orbit with the position of a drag-perturbed satellite that was initially in the same circular orbit (and at the same position) as the drag-free body. At the time when the drag is "turned-on," the drag-perturbed satellite departs from the circular orbit and initially assumes a smaller angular velocity than the drag-free satellite, thereby falling behind the drag-free satellite in angular position. Because of the conservation of angular momentum, the angular velocity of the drag-perturbed satellite increases as its altitude decreases, and it overtakes the drag-free satellite in angular position. The angular position (measured from the position where the drag is turned on) at which the drag-perturbed satellite overtakes the drag-free satellite has been

shown in Ref. 1 to be independent of the drag force to first order and has a value of 0.292 revolutions $\approx 105^\circ$.

The purpose of this note is to find the "catch-up" angular position when the perturbing force is an instantaneous velocity addition (ΔV) applied parallel and opposite in direction to the circular velocity. Results show that the catch-up angular position (measured from the point of application of the ΔV) varies between 63.640° and 73.092° as the ΔV varies from circular velocity to zero.

Analysis

This analysis will define the catch-up point for the limiting cases where ΔV approaches zero and where ΔV approaches retrograde circular velocity. The method of calculating the catch-up point for other values of ΔV will be indicated.

If two bodies are traveling together in a circular orbit in an inverse-square force field, and one of the bodies is perturbed by a ΔV parallel to its velocity vector, that body will enter an ellipse (assuming ΔV is not sufficient to cause escape) that is tangent to the original circle. One apse of the ellipse will be at a distance r (the original circular orbit radius) from the force center, and the other apse will be at a distance of $r \pm \Delta r$, where $+$ implies a ΔV along the circular velocity vector, and $-$ implies a ΔV opposite to the circular velocity vector. The semimajor axis and eccentricity for the new ellipse are given, respectively, by

$$a = r [1 \pm \chi] \\ e = \chi / [1 \pm \chi] \quad (1)$$

where $\chi = \Delta r / 2r$. From the vis-viva equation,

$$\frac{\Delta V}{V} = \left| 1 - \left(\frac{1 \pm 2\chi}{1 \pm \chi} \right)^{1/2} \right| \quad (2)$$

If the ΔV is applied to the circular velocity in a retrosense, the minus signs apply in Eqs. (1) and (2). Let θ_E be the angular travel of the body in the ellipse, and let θ be the angular travel of the body in the circle, both measured from the point of application of the retrograde ΔV . The true anomaly of the body in the ellipse is then

$$v = \pi + \theta_E \quad (3)$$

and the mean anomaly is

$$M = \frac{\mu^{1/2}}{a^{3/2}} \left[\frac{\pi a^{3/2}}{\mu^{1/2}} + \frac{r^{3/2} \theta_E}{\mu^{1/2}} \right] \quad (4)$$

where

$$\begin{aligned} \mu &= \text{gravitational constant} \\ \mu^{1/2} / a^{3/2} &= \text{mean motion of the body in the ellipse} \\ \pi a^{3/2} / \mu^{1/2} &= \text{half of the period of the body in the ellipse} \\ (r^{3/2} / \mu^{1/2}) \theta &= \text{time measured from apogee} \end{aligned}$$

Using Eq. (1) in (4) and simplifying gives

$$M = \pi + [\theta / (1 - \chi)^{3/2}] \quad (5)$$

Reference 2 (p. 171) gives the relation between v and M in an ellipse as

$$v = M + e \sin M + \frac{5}{4} e^2 \sin 2M + 0(e^3) \quad (6)$$

Substituting (1), (3), and (5) into (6) and expanding in power of χ gives

$$\begin{aligned} \pi + \theta_E = \pi + \theta [1 + \frac{3}{2}\chi + 0(\chi^2)] + \\ 2\chi [1 + \chi + 0(\chi^2)] \sin \{ \pi + \theta [1 + \frac{3}{2}\chi + \\ 0(\chi^2)] \} + 0(\chi^2) \end{aligned}$$

Now, setting $\theta_E = \theta$ and dividing through by χ yields

$$0 = \theta [\frac{3}{2} + 0(\chi)] - 2 [1 + 0(\chi)] \sin \{ \theta [1 + 0(\chi)] \} + 0(\chi)$$

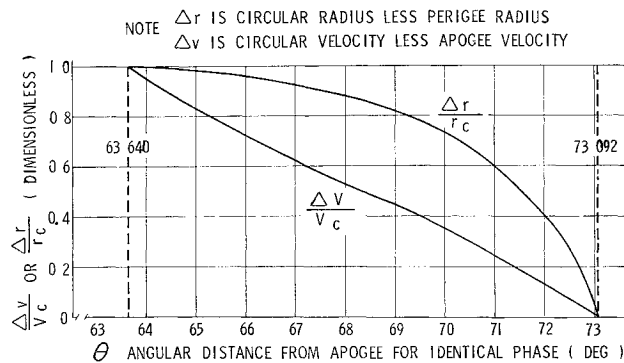


Fig 1 Location of "catch-up" point for retrograde ΔV

Taking the limit of the foregoing expression as $\chi = (\Delta r/2r) \rightarrow 0$ gives the following limiting catch-up point as $\Delta V \rightarrow 0$ †:

$$\theta_c = \frac{4}{3} \sin \theta \quad (7)$$

The solution of Eq (7) is $\theta = 73.092^\circ$. It can be easily shown that the same limit [Eq (7)] is reached when the ellipse is initially larger than the circle (i.e., ΔV is along the circular velocity in a positive sense) and is allowed to approach the circle.

As ΔV approaches retrograde circular velocity, the resulting ellipse approaches a rectilinear ellipse. The true anomaly in such a limiting ellipse approaches 180° at all points except at the force center where the rate of change of true anomaly approaches infinity. Therefore, for this case, the catch-up point will obviously occur when the perturbed body is at the force center. The time required for the body to reach the force center is one-half its period and is given by

$$t = \frac{\pi a^{3/2}}{\mu^{1/2}} = \frac{\pi (r_c/2)^{3/2}}{\mu^{1/2}} \quad (8)$$

During this time, the body in the circular orbit travels through an angle given by

$$\theta = (\mu^{1/2}/r^{3/2})t \quad (9)$$

Combining (8) and (9) and solving for θ yields

$$\theta = \pi/2^{3/2} \quad (10)$$

or

$$\theta = 63.640^\circ$$

The procedure for finding the catch-up point for a Δr (or ΔV) between the extremes just analyzed is first to estimate the catch-up θ_E and form the true anomaly of the ellipse [Eq (3)]. Next, the corresponding eccentric anomaly is found, and, consequently, the time from apogee is found from an appropriate form of Kepler's equation. The circular travel θ is then found from (9), and the difference $(\theta - \theta_E)$ is added to the original estimate of θ_E to form a new estimate. The process is repeated until $(\theta - \theta_E)$ is sufficiently small to be called zero.

Figure 1 is a plot of the angular distance from apogee of the catch-up points as functions of $(\Delta r/r)$ and $(\Delta V/V)$ for retrograde ΔV 's.

References

- 1 Karrenberg, H. K., Levin, E., and Lewis, D. H., "Variation of satellite position with uncertainties in the mean atmospheric density," ARSJ 32, 576-582 (1962).
- 2 Moulton, F. R., *An Introduction to Celestial Mechanics* (The MacMillan Co., New York, 1914), pp. 169-171.

† It can be seen from Eq (2) that, for small χ , $\Delta V/V_c \approx \pm \chi/2 = \pm \Delta r/4r_c$ and therefore $\Delta V \rightarrow 0$ as $\chi \rightarrow 0$.

Drag Minimization Using Exact Methods

SIDNEY A. POWERS*

Northrop Corporation, Hawthorne, Calif

A method of determining optimum solutions to nonlinear problems has been used to determine a minimum drag body of revolution for $M = 7$ at sea level. It is shown that the drag of the basic spherical- $\frac{3}{4}$ power-law body can be reduced significantly by using a very small sphere and making the body somewhat "fatter" than a $\frac{3}{4}$ power-law body.

A METHOD of treating nonlinear optimization problems has been discussed previously in detail in Ref. 1. This method is applied here to the problem of determining the minimum drag body of revolution for a freestream Mach number of 7.0 at sea level. The flow field is taken as inviscid and in chemical equilibrium.

The configuration is required to have a nominal fineness ratio of 4.0 and a spherical nose. The optimum size of the hemisphere and the contour of the afterbody are to be determined. As a "basic" shape, a body of unit length was used which had a sphere tangent to a $\frac{3}{4}$ power-law afterbody at the 0.05 body length point.

Between the sphere-body tangency point and the body base, a polynomial perturbation was added to the basic body:

$$\Delta y = A\xi^4 + B\xi^3 + C\xi^2 + D\xi + E \quad (1)$$

where

$$\xi = (X - X_T)/(X_m - X_T)$$

and X_T is the sphere-body tangency point. The following boundary conditions were imposed on Eq (1):

$$\begin{aligned} \Delta y &= 0 & \text{at } \xi &= 0 \\ \Delta y &= 0 & \text{at } \xi &= 1 \\ \Delta y' &= 0 & \text{at } \xi &= 0 \end{aligned}$$

Reference 2 describes in detail the method of determining the functional relation of drag on the sphere-body tangency point and the perturbation polynomial. Briefly, the boundary conditions just given make it possible to split the perturbation

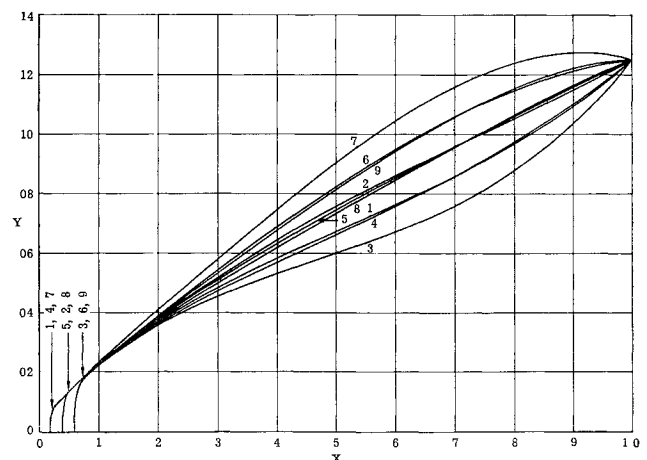


Fig 1 Body shapes specified by the Latin Square

Received September 23, 1963; revision received January 29, 1964

* Member of Technical Management Gas Dynamics Branch, Norair Division. Member AIAA.